GPC light shaper: static and dynamic experimental demonstrations.

Bañas, Andrew Rafael; Kopylov, Oleksii; Villangca, Mark Jayson; Palima, Darwin; Glückstad, Jesper

Published in:
Optics Express

Link to article, DOI:
10.1364/OE.22.023759

Publication date:
2014

Document Version
Publisher's PDF, also known as Version of record

GPC light shaper: static and dynamic experimental demonstrations

Andrew Bañas, Oleksii Kopylov, Mark Villangca, Darwin Palima, and Jesper Glückstad*

DTU Fotonik, Dept. Photonics Engineering, Ørsted Plads 343, Technical University of Denmark, DK-2800 Kgs. Lyngby, Denmark

*jesper.gluckstad@fotonik.dtu.dk

http://www.ppo.dk

Abstract: Generalized Phase Contrast (GPC) is an efficient method for generating speckle-free contiguous optical distributions useful in diverse applications such as static beam shaping, optical manipulation and, recently, for excitation in two-photon optogenetics. GPC allows efficient utilization of typical Gaussian lasers in such applications using binary-only phase modulation. In this work, we experimentally verify previously derived conditions for photon-efficient light shaping with GPC [Opt. Express **22**(5), 5299 (2014)]. We demonstrate a compact implementation of GPC for creating practical illumination shapes that can find use in light-efficient industrial or commercial applications. Using a dynamic spatial light modulator, we also show simple and efficient beam shaping of reconfigurable shapes geared towards materials processing, biophotonics research and other contemporary applications. Our experiments give ~80% efficiency, ~3x intensity gain, and ~90% energy savings which are in good agreement with previous theoretical estimations.

OCIS codes: (070.6110) Spatial filtering; (070.0070) Fourier optics and signal processing; (120.5060) Phase modulation; (140.3300) Laser beam shaping.

References and links

1. D. Palima, A. R. Bañas, G. Vizsnyiczai, L. Kelemen, P. Ormos, and J. Glückstad, "Wave-guided optical waveguides," Opt. Express **20**(3), 2004–2014 (2012).
2. Y. Hayasaki, T. Sugimoto, A. Takita, and N. Nishida, "Variable holographic femtosecond laser processing by use of a spatial light modulator," Appl. Phys. Lett. **87**(3), 031101 (2005).
3. E. Papagiakoumou, F. Anselmi, A. Bègue, V. de Sars, J. Glückstad, E. Y. Isacoff, and V. Emiliani, "Scanless two-photon excitation of channelrhodopsin-2," Nat. Methods **7**(10), 848–854 (2010).
4. E. Papagiakoumou, "Optical developments for optogenetics," Biol. Cell **105**(10), 443–464 (2013).
5. D. Palima, C. A. Alonzo, P. J. Rodrigo, and J. Glückstad, "Generalized phase contrast matched to Gaussian illumination," Opt. Express **15**(19), 11971–11977 (2007).
6. T. R. M. Sales, "Structured microlens arrays for beam shaping," Proc. SPIE **5175**, 109–120 (2003).
7. C. Kopp, L. Ravel, and P. Meyrueis, "Efficient beamshaper homogenizer design combining diffractive optical elements, microlens array and random phase plate," J. Opt. A, Pure Appl. Opt. **1**(3), 398–403 (1999).
8. J. A. Hoffnagle and C. M. Jefferson, "Design and performance of a refractive optical system that converts a Gaussian to a flattop beam," Appl. Opt. **39**(30), 5488–5499 (2000).
9. W. B. Veldkamp, "Laser beam profile shaping with interlaced binary diffraction gratings," Appl. Opt. **21**(17), 3209–3212 (1982).
10. M. R. Wang, "Analysis and optimization on single-zone binary flat-top beam shaper," Opt. Eng. **42**(11), 3106 (2003).
11. A. Bañas, D. Palima, M. Villangca, T. Aabo, and J. Glückstad, "GPC light shaper for speckle-free one- and two-photon contiguous pattern excitation," Opt. Express **22**(5), 5299–5311 (2014).
12. A. W. Lohmann and D. P. Paris, "Binary fraunhofer holograms, generated by computer," Appl. Opt. **6**(10), 1739–1748 (1967).
13. W. H. Lee, "Sampled Fourier transform hologram generated by computer," Appl. Opt. **9**(3), 639–643 (1970).
14. J. Glückstad and D. Z. Palima, *Generalized Phase Contrast: Applications in Optics and Photonics*, Springer Series in Optical Sciences (Springer, 2009).

#217181 - $15.00 USD Received 16 Jul 2014; revised 11 Sep 2014; accepted 12 Sep 2014; published 22 Sep 2014

15. L. Ge, M. Duelli, and R. Cohn, "Enumeration of illumination and scanning modes from real-time spatial light modulators," Opt. Express **7**(12), 403–416 (2000).
16. T. Matsuoka, M. Nishi, M. Sakakura, K. Miura, K. Hirao, D. Palima, S. Tauro, A. Bañas, and J. Glückstad, "Functionalized 2PP structures for the BioPhotonics Workstation," Prof. SPIE **7950**, 79500Q (2011).
17. D. Palima and J. Glückstad, "Multi-wavelength spatial light shaping using generalized phase contrast," Opt. Express **16**(2), 1331–1342 (2008).
18. J. Glückstad and P. C. Mogensen, "Reconfigurable ternary-phase array illuminator based on the generalised phase contrast method," Opt. Commun. **173**, 169–175 (2000).
19. S. Tauro, A. Bañas, D. Palima, and J. Glückstad, "Experimental demonstration of Generalized Phase Contrast based Gaussian beam-shaper," Opt. Express **19**(8), 7106–7111 (2011).
20. M. Villangca, A. Bañas, O. Kopylov, D. Palima, and J. Glückstad, "GPC-enhanced read-out of holograms," Submitted to Opt. Express (2014).
21. V. Daria, J. Glückstad, P. C. Mogensen, R. L. Eriksen, and S. Sinzinger, "Implementing the generalized phase-contrast method in a planar-integrated micro-optics platform," Opt. Lett. **27**(11), 945–947 (2002).
22. D. Palima and J. Glückstad, "Gaussian to uniform intensity shaper based on generalized phase contrast," Opt. Express **16**(3), 1507–1516 (2008).

1. Introduction

Light shaping is relevant to both research and industry. This is especially the case with lasers. Hence, photon efficient light shaping, typically using phase-only methods, are extensively applied in research such as for advanced microscopy, optical manipulation [1], materials processing [2], and, more recently, for neurophotonics and two-photon optogenetics [3]. Outside the laboratory, efficient light shaping is also desirable for applications such as laser machining, photolithography and video displays to name a few. These diverse applications would require light to be shaped in different ways. For example, the illuminated surfaces of spatial light modulators (SLMs), used in both optics research and consumer display projectors, have a rectangular form factor. A variety of shapes bounded by steep edges are desirable in laser cutting or engraving. In two-photon optogenetics research [4], one would like to selectively illuminate intricate patterns of dendrites or axons within neurons, preferably with minimal noise or speckles.

On the other hand, laser sources typically have limited shapes, a common example being the TEM_{00} or Gaussian profile. Simply placing a shaped aperture over a Gaussian beam, i.e. amplitude modulation, is inefficient. For example, around 70% or more of the incident power can be lost when illuminating a rectangle with an expanded Gaussian beam [5]. To complicate matters, this wasted power could contribute to device heating, which can either shorten the device lifespan or require even more power if active cooling is employed. Besides the obvious disadvantages of inefficiency, the high price tag of advanced laser sources demands an efficient way of managing their available photons.

1.1 Photon-efficient static light shaping

Several solutions based on non-absorbing or phase-only methods exist for the efficient transformation of a Gaussian beam into rectangular, circular or other simple patterns. Static beam shapers such as engineered diffusers, microlens arrays or homogenizers [6,7] suffer from speckled or grainy output intensities. Refractive mapping [8] requires specially fabricated aspheric lenses, making it hard to adapt to different shapes. Diffractive optical elements or phase plates [9,10] alter the phase of a Gaussian beam such that it becomes a rectangle or circle in the far field or after an additional lens. These approaches can suffer from convolution effects that blur the edges of the shaped output and are generally speckled.

GPC shapes light using a direct phase to intensity mapping. A phase-only aperture directly representing the desired output intensity is imaged through its interference with a synthetic reference wave (SRW). This common path mapping configuration renders steep well-defined edges in the shaped intensity output. The SRW is formed by phase shifting the lower spatial frequencies through a phase contrast filter (PCF) at the Fourier plane (Fig. 1). GPC could thus be implemented with easily mass produced binary phase plates as will be demonstrated in our experiments. Phase masks and PCFs can also be implemented in a number of alternative ways

#217181 - $15.00 USD Received 16 Jul 2014; revised 11 Sep 2014; accepted 12 Sep 2014; published 22 Sep 2014

such as a hole in a piece of glass with a controlled thickness or as a bump or depression on a reflective surface. Techniques used for single-mode fibers can also be adopted if dealing with high power lasers. Furthermore, the target output shapes could easily be replaced without increasing the fabrication cost or complexity.

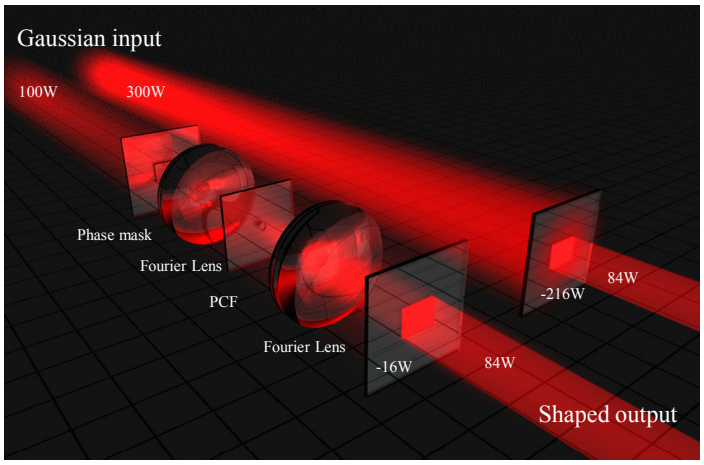

Fig. 1. Side-by-side comparison of a GPC light shaper (left) and amplitude masking (right), illuminated with similarly collimated Gaussian beams. For the same output, the GPC LS, being 84% efficient, requires only 1/3 incident power compared to the 28% efficient amplitude mask. This saves up to 93% of typical amplitude masking losses. The GPC LS is constructed using a 4*f* imaging lens setup, a binary phase mask at the input and a phase contrast filter at the Fourier plane.

1.2 Replacing amplitude modulation

Despite its obvious inefficiency, the use of hard truncation or amplitude modulation persists because of its low cost, simplicity and the quality of the output beam. Many of the advantages of amplitude modulation are also shared by GPC in phase modulation. Both are characterized by sharply outlined patterns with contiguous phase and intensity. Both techniques are also easily adapted to more arbitrary or complex light patterns. The main difference is the efficiency. Our calculations in [11] show that GPC's efficiency is typically around ~84%. On the other hand, amplitude modulation typically has a low efficiency, directly proportional to the encoded pattern's fill factor and also dependent on the modulating device (e.g. LCoS or DMD). For similar illumination patterns we have compared, the efficiencies of amplitude modulation are around ~28% at best. The threefold intensity gain of GPC means that less powerful lasers can be used for the same application. This can be highly important when one is already exhausting the full power of the installed laser and getting higher power would come at an appreciable cost or, worse, it might not be commercially available and still under development. Furthermore, the combined effects of GPC's efficiency and intensity gain enables it to save up to ~93% of typical amplitude masking losses [11]. These quantitative comparisons are illustrated in Fig. 1, wherein both methods are used to deliver 84W through identical rectangles.

1.3 Dynamic light shaping

Dynamic light shaping using spatial light modulators enables the efficient generation of programmable and arbitrary light intensity patterns. Hence it is widely used in research such as machine vision, optical trapping and manipulation, and for two-photon optogenetics. In materials processing, there is also a growing interest in using single shot 2D patterns or specially shaped scanning beams. Depending on the requirements, digital holography (DH) [12,13] and GPC [14] have been the main options for phase-only beam shaping. While DH is

#217181 - $15.00 USD Received 16 Jul 2014; revised 11 Sep 2014; accepted 12 Sep 2014; published 22 Sep 2014

ideal for diffraction-limited 3D spot distributions, GPC is particularly advantageous in generating speckle-free contiguous light patterns. When using DH, differing output phase values and overlapping point spread functions result in speckles or noise-like features [15] that prevent high-fidelity contiguous light distributions. In particular, the intensity fluctuations due to these inherent speckles become a problem when they are enhanced by two-photon excitation such as in direct laser writing [16] or in two-photon optogenetics [4]. Moreover, GPC is typically used in a simple imaging geometry thereby avoiding dispersion effects that would be inherently present in the focusing geometry of DH. This makes GPC advantageous for use with multiple wavelengths [17] or in temporal focusing [3,4].

We thus show static and dynamic GPC light shaper demonstrations in Sections 5 and 6. But before we proceed to experiments, we briefly review the optimization of GPC for reshaping Gaussian illumination in Section 2. We also analyze the tolerances of the PCF's placement and phase shifts in Section 3, and then propose a method for experimentally calibrating the PCF's axial placement in Section 4.

2. Reshaping Gaussian beams with GPC

When building a GPC system, it is first necessary to determine the best choice of phase mask and PCF given the wavelength, beam diameter and other constraints. We therefore summarize how to choose optimal phase masks and PCF sizes based on the formulations in [11] – all currently based on π-shifting phase values. Given a Gaussian beam with a $1/e^2$ radius, w_0, illuminating a phase mask with phase profile $\phi(x,y)$, we define its normalized Fourier zero order, $\bar{\alpha}$, as

$$\bar{\alpha} = \frac{1}{\pi w_0^2}\iint \exp\left[-\left(x^2+y^2\right)/w_0^2\right]\exp\left[i\phi(x,y)\right]dxdy \ . \tag{1}$$

In the absence of an input phase mask, the input Gaussian would be focused into another Gaussian at the Fourier plane. Assuming a wavelength, λ, and focal length, f, the Gaussian waist radius at the Fourier plane, w_f, is given by

$$w_f = \lambda f/(\pi w_0). \tag{2}$$

The phase contrast filter's π-shifting region's radius, Δr_f, is measured relative to this Fourier Gaussian, and is characterized by the dimensionless η given by

$$\eta = \Delta r_f / w_f \tag{3}$$

By imposing amplitude matching with the synthetic reference wave [5], and that Δr_f coincides with the Fourier distribution's zero crossing [11], the conditions for optimal contrast and efficiency of the GPC output lead to the following equations

$$\eta = \sqrt{-\ln\left(1-\sqrt{1/2}\right)} = 1.1081, \tag{4}$$

$$\bar{\alpha} = \sqrt{1/2} = 0.7071. \tag{5}$$

Equations (4) and (5) summarize the conditions for an optimally performing GPC system under Gaussian illumination. The fixed value for η in Eq. (4) means that a reconfigurable GPC system with a fixed PCF will consistently perform optimally with different phase masks satisfying Eq. (5). The phase mask's geometry, $\phi(x,y)$, should thus be tweaked such that Eq. (5) is satisfied. For simple shapes such as a circle and a rectangle, we have analytically shown how to scale $\phi(x,y)$ such that $\bar{\alpha} = \sqrt{1/2}$ [11]. We show how these conditions are used for fabricating static glass filters in Section 5, and for programming a dynamic SLM in Section 6.

#217181 - $15.00 USD Received 16 Jul 2014; revised 11 Sep 2014; accepted 12 Sep 2014; published 22 Sep 2014

But before that, we also tackle practical experimental issues that include the identification of tolerance regimes of a practical GPC system and the development of a technique for fine-tuning of the PCF's position using destructive interference.

3. Tolerances of some critical parameters

In numerical simulations, there is no worry for alignment, exact placement of components, dirt, nonlinearities and such variations, which are always present in actual experiments. There are arguably countless parameters to consider in a real setup but, among them, the PCF is one with little room for error. Both PCF and the Fourier focal spot are typically in the micron range. Misaligning these two could effectively remove the PCF and revert a GPC phase imaging system to a normal 4*f* telescopic setup. We consider here some parameters that are crucial in our experiments and fabrication process, namely, the PCF's displacement and the effective phase shift of the phase mask and PCF.

3.1 PCF displacements

We numerically simulate typical PCF misalignment situations, i.e. axial displacements along the optical axis, and lateral displacements along the Fourier plane. The phase mask shapes considered are a circle, a square and a rectangle with 4:3 aspect ratio. Efficiencies and energy savings are evaluated at different displacements (Fig. 2). The energy savings tells how much energy is saved compared to a beam that is hard truncated to a similar geometry, with the incident power increased to give the same output brightness as GPC. The displacements are expressed relative to the PCF size or focal length, and also in relation to a GPC light shaper (LS) designed for λ = 750nm, $2w_0$ = 1mm, and with f = 50mm Fourier lenses as in the experiments.

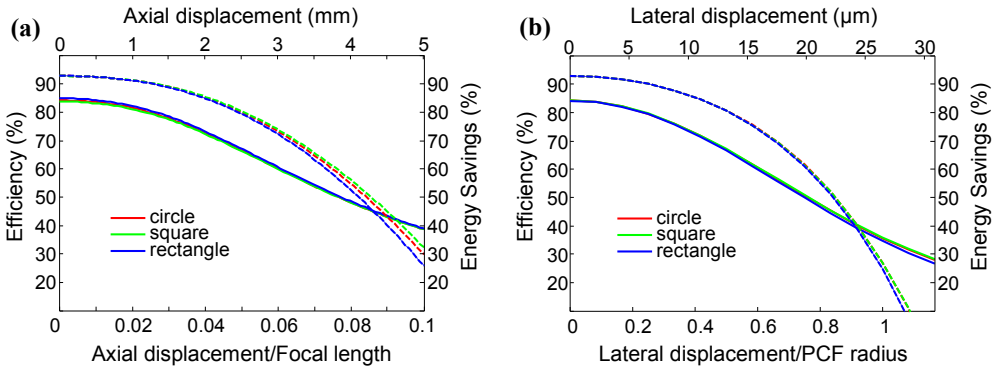

Fig. 2. Tolerance of the PCF's positioning. The efficiency (solid lines) and energy savings (broken lines) are evaluated at different axial (a) and lateral (b) displacements.

Along the axial direction, the efficiency stays at above 80% if the PCF does not go beyond ~2% of the focal length (~1.2mm). Energy savings is slightly more robust allowing about ~2.5mm axial displacement before the 80% cutoff. Lateral displacements are more critical owing to the small size of the PCF. For the GPC LS considered having a PCF radius of 26.5μm, lateral displacements can go only up to ~5 and ~12 microns before the efficiency and energy savings, respectively, go below 80%.

3.2 Phase mask and PCF phase shift variations

We now consider the effect when the input phase mask and the PCF phase shift deviate from π. This deviation can arise due to expected variations in feature depths during the fabrication process, such as wet etching. Again, we evaluate efficiency and energy savings for different

#217181 - $15.00 USD Received 16 Jul 2014; revised 11 Sep 2014; accepted 12 Sep 2014; published 22 Sep 2014

shapes. But since the differences are subtle, we only show the results for a 4:3 rectangular phase mask.

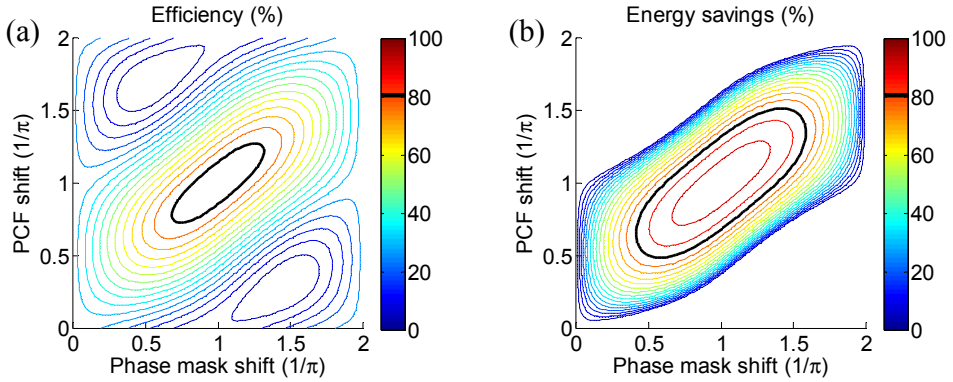

Fig. 3. Contour plots showing the efficiency (a) and energy savings (b) of a GPC LS using a 4:3 rectangular phase mask. A black contour line is drawn around the region for which efficiency or energy savings are at least 80%.

The diagonal orientation of the elliptically shaped regions of high efficiency and high energy savings (c.p. Fig. 3) implies that the GPC LS is more robust to phase shift errors when both phase mask and PCF have the same phase shift (a similar result has also been derived for plane-wave illuminated GPC [18]). This can happen when the phase mask and PCF are uniformly etched on the same wafer. Under this condition, phase shift variations of up to ~20% are still tolerable, as shown by the black contour line representing 80% efficiency. For 80% energy savings, the phase shift deviation can reach up to 50%.

4. Axial calibration of the PCF using a darkness phase mask

To aid in the positioning of the PCF, we devised a calibration procedure that is less prone to false positive measurements. Normally, GPC is designed such that constructive interference occurs at the foreground. However, measuring the optimal brightness is not as straightforward without, first, setting a reference. By changing the foreground's fill factor relative to the Gaussian illumination, GPC can also generate darkness at the output via destructive interference. For a π-phase shifting circle phase mask, we found numerically that darkness is generated when the phase mask radius is ~1.02 times the Gaussian $1/e^2$ radius. It is also possible to use a truncating iris, and we find that darkness is generated at an aperture radius of about ~$0.83w_0$. Although an amplitude truncating iris has the advantage of being wavelength independent, it is much easier to work with a transparent phase-only darkness mask as transmitted peripheral light can help during alignment. Furthermore, a phase-only mask can be fabricated on the same wafer containing the normal phase masks and PCFs, making it economical. Figure 4 shows GPC simulations using a darkness phase mask together with an image captured in our experimental calibration after the PCF was aligned. The input phase mask can then be replaced with the desired pattern afterwards.

#217181 - $15.00 USD Received 16 Jul 2014; revised 11 Sep 2014; accepted 12 Sep 2014; published 22 Sep 2014

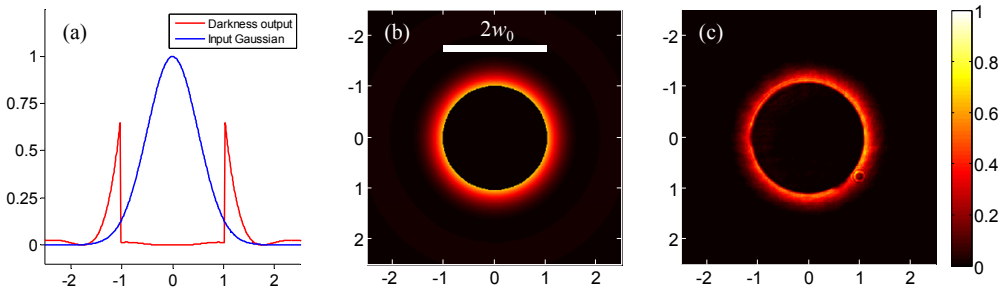

Fig. 4. Relative intensity of a GPC generated darkness compared to the input Gaussian (a). Intensity profiles obtained from a simulation (b) and from experiment (c). This darkness condition is a convenient indicator of correct PCF alignment.

5. Static light shaping experiments

5.1 Construction of a pen sized GPC LS

The GPC LS used for our static experiments was designed to interface directly with the output of laser sources. Commercial lasers typically have beam diameters of around ~1mm to ~5mm. Using two f = 50mm Fourier lenses allowed us to keep the setup compact. This also kept the PCF at a size that is still manageable with wet etching and off-the-shelf optics assembly. The GPC LS assembled with Thorlabs's half-inch optics and 16mm cage components is shown in Fig. 5. Its overall length is just a little over $3f$ = 150mm, which is around the size of a pen. This is significantly smaller than our previous proof-of-principle Gaussian GPC demonstration with $3f$ = 600mm [19]. The minimal footprint thus allows the GPC LS to be conveniently added to existing laser shaping experiments [20]. For more compact implementations, such as for OEM use, integrated micro-optics platforms [21] or alternative fabrication and assembly techniques can also be adopted.

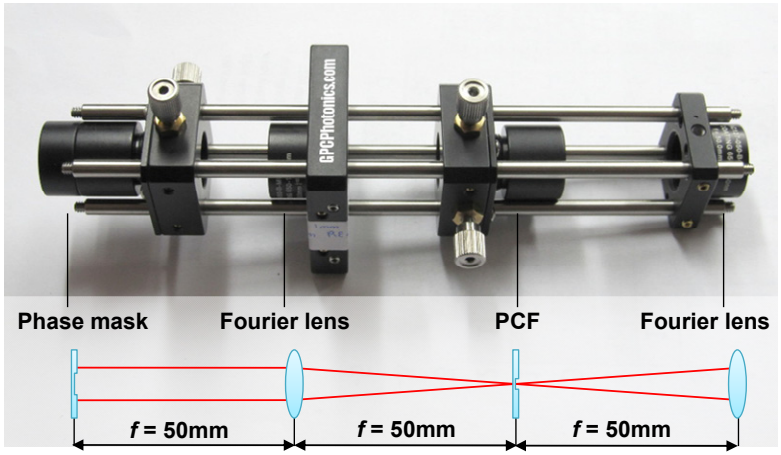

Fig. 5. Pen sized GPC LS using two f = 50mm Fourier lenses and half inch optics assembly.

We designed the phase mask and PCF for use with $2w_0$ = 1mm, λ = 750nm and f = 50mm. The material used is fused silica (n = 1.454 at λ = 750nm). After photolithographic transfer, the patterns are etched to a depth of ~826nm to give a π phase difference relative to the un-etched surroundings. The PCF radius is calculated using Eqs. (3) and (4), hence,

$$\Delta r_f = \eta \frac{\lambda f}{\pi w_0} = \frac{1.1081 \times 0.75\mu m \times 50mm}{\pi \times 0.5mm} = 26.5\mu m \qquad (6)$$

#217181 - $15.00 USD Received 16 Jul 2014; revised 11 Sep 2014; accepted 12 Sep 2014; published 22 Sep 2014

The size of the phase mask that satisfies Eq. (5) has a less straightforward derivation. For circles or rectangles, the phase mask size relative to the Gaussian beam diameter can be obtained from the tabulated ζ or ζ_{Rect} values in [11]. As an example, for a rectangular phase mask with aspect ratio 4:3, the width has to be 0.4087 (ζ_{Rect}) times the beam diameter.

$$W = \zeta_{\text{Rect}} \times (2w_0) = 0.4087 \times 1\text{mm} = 408.7\mu\text{m} \tag{7}$$

The height, H, is then obtained from the width and aspect ratio (note: $H \le W$, as typical to video displays).

$$H = \frac{3}{4}W = 306.5\mu\text{m} \tag{8}$$

The phase masks and PCFs are diced such that they can be fitted into half-inch optics mounts. The size of the circular and square phase masks are obtained in a similar manner. The ζ or ζ_{Rect} for these shapes are included on Table 1 together with the summary of experimental results. During assembly, we utilized the phase-only darkness calibration masks to fine tune the axial placement of the PCF. These masks were fabricated with a radius of 510μm.

Table 1. Experimentally Measured Efficiency, Intensity Gain and Energy Savings of GPC Shaped Light Compared with a Hard Truncated or Amplitude Masked Gaussian for a Circle and Different Rectangles

Shape or aspect ratio	ζ or ζ_{Rect}	Width or Diameter (μm)	GPC eff (%)	GPC gain	Amp masking eff (%)	E. savings (%)
Circle	0.3979	397.9	81.28	2.89	28.15	90.98
Square	0.3533	353.3	76.34	2.73	27.97	87.96
4:3	0.4087	408.7	82.41	2.91	28.31	91.57

5.2 Static light shaping results

For our laser source, we used a supercontinuum laser from NKT Photonics that has a 1mm beam diameter. This enables us to conveniently test different wavelengths by inserting a color filter, instead of replacing the entire laser. In our measurements, we used a 750nm bandpass filter from Thorlabs with a bandwidth of 10nm. This laser source is directed to the GPC LS using some relay mirrors that also provided beam alignment. Output from the GPC LS is magnified (2x) then recorded into a beam profiler (Gentec-EO).

Different GPC output shapes were tested on the same GPC LS by interchanging the phase masks. We have listed the measured efficiencies, gain and energy savings for different shapes in Table 1. To rule out reflection losses, we used a reference Gaussian that is obtained when the PCF is misaligned and the phase mask is removed. We averaged this Gaussian from 3 measurements.

Figures 6(a)–6(c) show GPC outputs for a circle, a square and a rectangle with 4:3 aspect ratio masks using optimized parameters listed in Table 1. The corresponding efficiencies, gain and energy savings are also shown for each shape and are consistently around ~80%, ~3x and ~90% respectively. The corresponding line scans are shown in Figs. 6(d) and 6(e). Two output measurements were taken (red and green plots) and measured against the reference Gaussian (blue plot). A calculated Gaussian fit (magenta) is used to normalize the axes in Fig. 6. There is an observable intensity roll off in the GPC output, but this is flatter than what can be attained from a hard truncated Gaussian [5]. If a flatter intensity is critical, a phase mask with an intensity compensating curvature [22] may be used with the GPC LS. Compared to previously reported efficiencies of ~75% [19], the use of optimization Eqs. (4) and (5) and the new darkness calibration procedure evidently contributed to raising the efficiency.

#217181 - $15.00 USD Received 16 Jul 2014; revised 11 Sep 2014; accepted 12 Sep 2014; published 22 Sep 2014

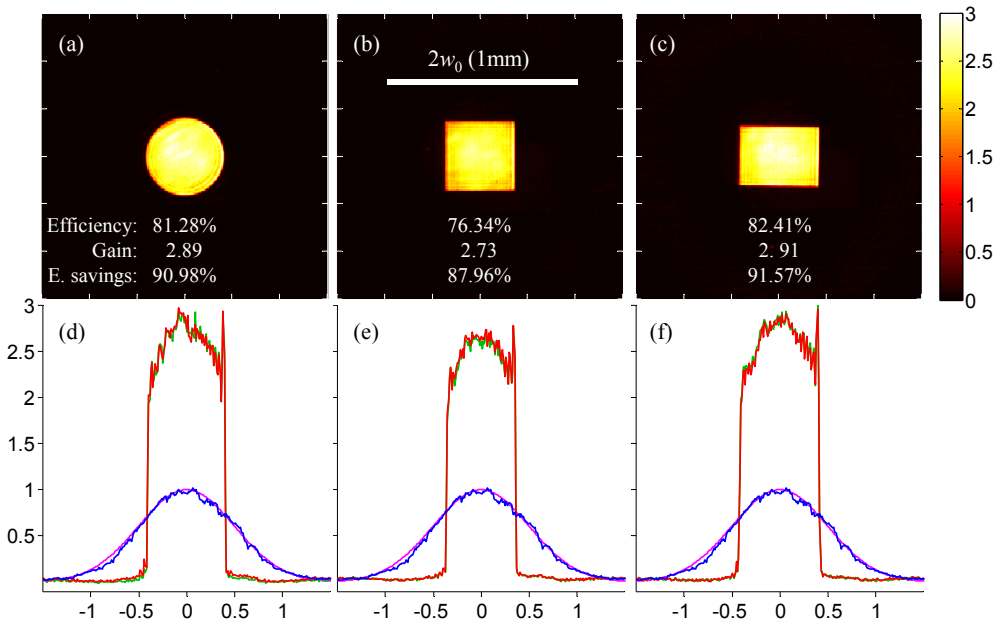

Fig. 6. GPC intensity outputs for a circle (a), a square (b), and a 4:3 rectangle (c) phase mask. The scale bar in (b) is twice the $1/e^2$ Gaussian waist, and tick marks in (a)-(c) are separated by half the Gaussian waist. Efficiencies, gain and energy savings are also shown, and are consistently around ~80%, ~3x and ~90% respectively. The corresponding intensity line scans are shown in (d)-(f). The axes are normalized relative to a reference Gaussian and tick marks are spaced $w_0/2$ (0.25mm) apart.

6. Arbitrary patterns formed with a dynamic phase-only spatial light modulator

We now show how GPC is applied for dynamic light shaping of speckle-free contiguous patterns. The setup used for generating arbitrary GPC output shapes is shown in Fig. 7.

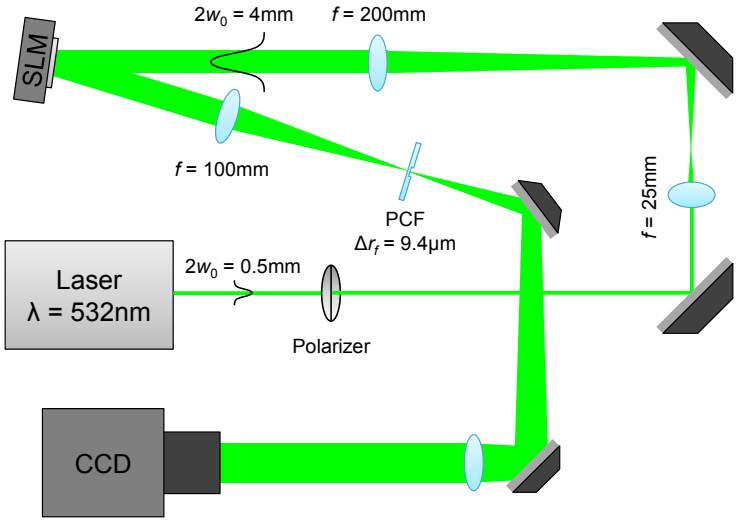

Fig. 7. GPC LS setup with Gaussian illumination on a dynamic spatial light modulator (SLM). The SLM is illuminated with horizontally polarized light and with $2w_0$ = 4mm. The phase on the SLM is passed through a GPC system using an f = 100mm and f = 150mm Fourier lenses, then imaged into a CCD camera.

#217181 - $15.00 USD Received 16 Jul 2014; revised 11 Sep 2014; accepted 12 Sep 2014; published 22 Sep 2014

We used an SLM (Hamamatsu Photonics) that has an area of 16 × 12mm^2 and pixel pitch of 20 microns. The SLM was illuminated with a 532nm diode laser module (Odicforce), horizontally polarized and expanded such that $2w_0$ = 4mm (200 SLM pixels). The Fourier lens used has a focal length of 100mm. Here, we used a PCF with Δr_f = 9.4μm which is relatively small due to the larger area of the SLM. When compactness is not a requirement, longer focal lengths can be used to minimize the focused light-intensity at the PCF and improve alignment and fabrication tolerances.

6.1 Optimally scaled arbitrary patterns

Binary bitmap images, $b(x, y)$, were displayed on the SLM and mapped to 0 and π phase shifts. The images were pre-scaled such that

$$\bar{\alpha} = 1 - 2\left\{\iint b(x,y)\exp\left[-\left(x^2+y^2\right)/w_0^2\right]dxdy\right\}/\pi w_0^2 = \sqrt{1/2}. \quad (9)$$

GPC results for various optimized images are shown in Fig. 8 together with the reference un-modulated Gaussian (Fig. 8(a)).

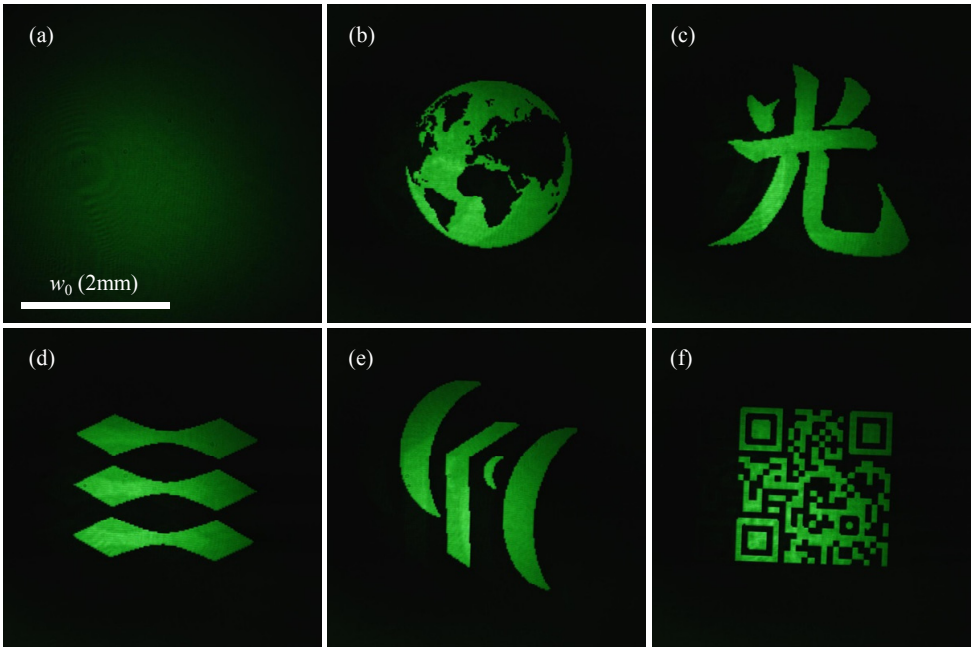

Fig. 8. Reference Gaussian (a) and GPC generated arbitrary patterns (b-f). GPC's ~3x gain makes the patterns noticeably brighter despite using the same laser power as the reference Gaussian. The patterns are scaled according to Eq. (9), then drawn on a phase-only SLM. A GPC LS after the SLM maps the phase patterns into intensity.

6.2 Dynamic and arbitrarily sized excitation patterns

When scaling of the light pattern is not an option, like in biological or optical manipulation experiments, $\bar{\alpha}$ is kept at its optimal value by addressing an additional outer phase ring such that Eq. (5) is still satisfied. The inner radius of the compensating ring, R_{comp}, is obtained using [11]

$$R_{\text{comp}} = w_0 \times \sqrt{-\ln\left[\left(1/2-\sqrt{1/8}\right)-\left\{\iint b(x,y)\exp\left[-\left(x^2+y^2\right)/w_0^2\right]dxdy\right\}/\pi w_0^2\right]}. \quad (10)$$

We have observed that the intensity beyond this radius is considerably lower than that in the utilized region due to the Gaussian roll-off. Hence, there is no need for a blocking mask as we

#217181 - $15.00 USD Received 16 Jul 2014; revised 11 Sep 2014; accepted 12 Sep 2014; published 22 Sep 2014

previously suggested in [11]. Results for the ring-compensated neuron-shaped patterns demonstrate GPC's ability to address multiple sites within a contiguous region in parallel without speckle noise (Fig. 9). Figures 9(d)–9(f) show the possibility to optimally illuminate a cell that is branching out.

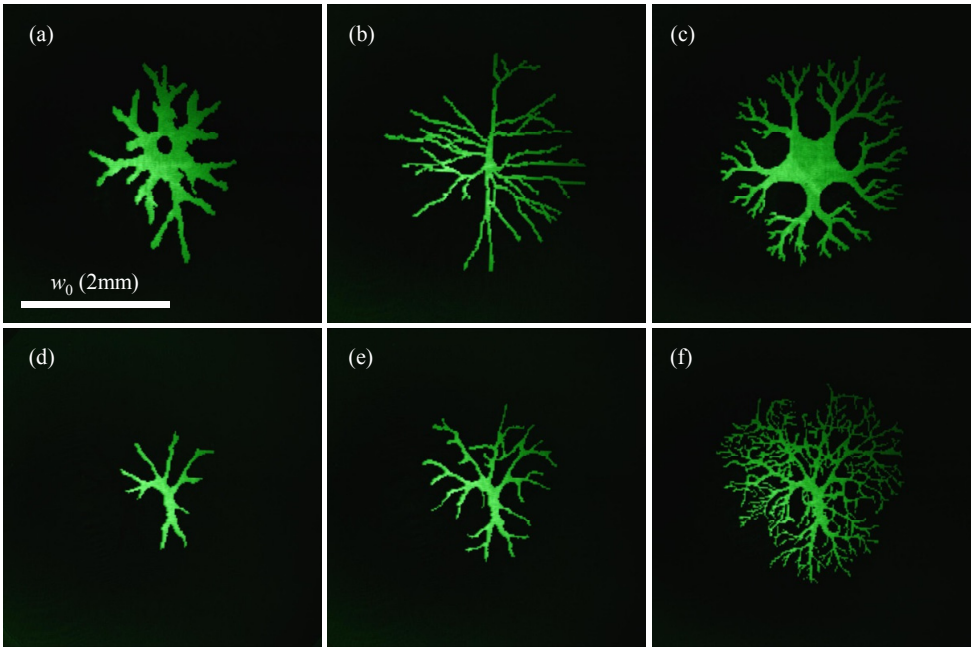

Fig. 9. (a)-(c) Intensity profiles of various neuron-inspired shapes, directly drawn without scaling, but α-compensated by an outer phase ring. (d)-(f) Snapshots from a pattern that is branching out (Media 1).

7. Summary and outlook

We have experimentally demonstrated efficient speckle-free light shaping using a GPC light shaper. Gaussian beams are transformed into a plurality of static illumination shapes or user-defined dynamic patterns. Results obtained from our previous work [11] simplify the task of implementing GPC for Gaussian illumination. We demonstrate these with circle, square and rectangle static phase masks and with more complex arbitrary and real-time dynamic shapes using an SLM. Our demonstrations show that a GPC LS could be re-used with a fixed PCF in tandem with a variety of interchangeable phase masks and still maintain desired efficiency and gain levels. Experiments show around ~80% efficiency, ~3x intensity gain and ~90% energy savings compared to the commonly implemented hard-truncated expanded Gaussian. The energy saved by using a GPC LS makes it attractive for many applications wherein light is best utilized in a particular shape, e.g. rectangles for SLM or display illumination, circles for laser materials processing or even intricate biological patterns found in neurophotonics research.

Acknowledgments

We thank the following for financial support: the Copenhagen Cleantech Cluster (CCC) for GAP funding and the Enhanced Spatial Light Control in Advanced Optical Fibres (e-space) project by the Danish Council for Strategic Research. We also thank our industrial collaborators, Hamamatsu Photonics K.K. Central Research Laboratory and NKT Photonics A/S. Finally, we thank Mr. Finn Pedersen for providing technical assistance in building our experimental setups.